Tribology Letters manuscript No.
(will be inserted by the editor)

On the contact area of nominally flat Hertzian contacts

Martin H. Müser

Received: date / Accepted: date

Abstract In a recent paper, Pastewka and Robbins, [Appl. Phys. Lett. (2016)], state an analytical expression for the real contact area of a Hertzian tip with small-scale roughness. We confirm that their formula predicts real contact areas quite well — with less than 10% error. Nonetheless, the complementary contact area does not show the proper scaling to the continuum results at large loads. This shortcoming is fixed in the present work by abandoning a mean-field approximation made in the original work. Analytical results can even be made essentially perfect with a relation giving the accurate dependence of contract area on pressure for contacts between solids with nominally flat surfaces.

Keywords Contact mechanics, Surface Roughness Analysis and Models

PACS 46.55.+d Tribology and mechanical contacts · 68.35.-p Solid surfaces and solid-solid interfaces: structure and energetics · 68.35.Gy Mechanical properties; surface strains

1 Introduction

Real contact areas are less than those perceived macroscopically due to the presence of small-scale roughness [3, 22]. The effect is now well described by Persson's contact mechanics theory [22,23], which merely requires one to compute a few well-defined, one-dimensional integrals for a given system. From their solution one can deduce not only contact areas and pressure distributions but also many other quantities such as the interfacial separation and its distribution [2], leakage [26,8] as well as statistical properties of the contact geometry [24,6]. Despite this progress, porting the insights gained for nominally flat surfaces to macroscopically curved surfaces has gained much less attention [18,20] than atomistic simulations addressing the question of how small-scale roughness affects the tribological behavior of tips scratching over a surface [29,15,17,7,11].

In a recent paper, Pastewka and Robbins [20] consider a non-adhesive Hertzian contact and add small-scale roughness to it. A central aspect of their work is the analysis of how true contact area depends on load in the absence of adhesion. They identify three regimes: at extremely small load, L, only one small-scale asperity is in contact with the counterface, in which case Hertzian contact mechanics holds, albeit with a small-scale radius of curvature. Near a cross-over load, L_c, for which Pastewka and Robbins provide accurate analytical estimates, the behavior crosses over to an intermediate regime, $A \propto L$. At large loads, Hertzian contact mechanics takes over again, this time with the "correct", macroscopic radius of curvature. For the last two regimes, Pastewka and Robbins derive accurate analytical relations despite using a mean-field approximation.

In this work, we drop the mean-field approximation made by Pastewka and Robbins [20] and investigate to what extent a more precise treatment improves the original relation. This is done by comparing our analytical expression to numerical data. Theory and numerical methods are described in sections 2 and 3, respectively. Results are presented in section 4. Conclusions are drawn in section 5.

Martin H. Müser
Department of Materials Science and Engineering
Saarland University, Campus
66123 Saarbrücken, Germany
E-mail: martin.mueser@mx.uni-saarland.de

2 Theory

According to Hertzian contact mechanics [10,13], the pressure profile in a contact of a rigid, parabolic tip with a flat, linearly elastic substrate is

$$p_{\rm H}(r) = p_0\sqrt{1-(r/a_0)^2}, \tag{1}$$

where r is the (in-plane) distance from the tip center, p_0 is the pressure in the tip center, and a_0 is the contact radius. The terms p_0 and a_0 satisfy

$$p_0 = \frac{3L}{2\pi a_0^2}, \tag{2}$$

$$a_0^3 = \frac{3LR}{4E^*}, \tag{3}$$

L being the mechanical load, R the tip's radius of curvature, and E^* the contact modulus.

Due to micro-scale roughness, real contact does not have to exist at every single point within the Hertzian contact radius. For macroscopically flat surfaces, the relative contact can be approximated quite well with the relation [22,27,30]

$$A_{\rm rel}^{\rm flat}(\bar p) \approx {\rm erf}\left(\frac{\sqrt{\pi}\kappa\bar p}{2E^*\bar g}\right) \tag{4}$$

$$\approx \frac{\kappa\bar p}{E^*\bar g} \quad \text{for} \quad \bar p \ll E^*\bar g. \tag{5}$$

Here $\bar p$ is the mean, macroscopic pressure, $\bar g$ is the root-mean-square slope of the (combined) surface roughness, and κ is a number, which turns out close to two for typical surface roughness [12,5,1,28,27].

In the philosophy of Persson theory [22,23,16], the real contact area can be estimated by first solving the problem macroscopically and then adding the effects of small-scale roughness locally. For the nominally flat Hertzian contact, this approach leads to the following estimate of the real contact area by integrating over the Hertzian contact area $A_{\rm H}$:

$$A_{\rm real} = \int_{A_{\rm H}} d^2r\, A_{\rm rel}^{\rm flat}\{p_{\rm H}(r)\}. \tag{6}$$

$$\approx \pi a_0^2 A_{\rm rel}(\bar p_{\rm H}), \tag{7}$$

The approximation (7) was made by Pastewka and Robbins [20]. In equation (6), they replaced the pressure profile from equation (1) with its mean value, $\bar p_{\rm H} \equiv \langle p(r)\rangle_{A_{\rm H}}$, averaged over the area $A_{\rm H}$,

$$\bar p_{\rm H} = \frac{L}{\pi a_0^2}. \tag{8}$$

Thus, the Pastewka-Robbins mean-field model yields

$$A_{\rm PR} = \pi a_0^2 {\rm erf}\left(\frac{\kappa L}{2\sqrt{\pi}E^*\bar g a_0^2}\right). \tag{9}$$

A supposedly better estimate can be found by abandoning the mean-field approximation to $p_{\rm H}(r)$ [16], which yields a first alternative model, specifically

$$\frac{A_{\rm I}(\kappa\tilde p)}{\pi a_0^2} = \left(1-\frac{1}{2\kappa^2\tilde p^2}\right){\rm erf}(\kappa\tilde p) + \frac{\exp\left(-\kappa^2\tilde p^2\right)}{\sqrt{\pi}\kappa\tilde p} \tag{10}$$

with

$$\tilde p = \frac{3L}{4\sqrt{\pi}E^*\bar g a_0^2} \tag{11}$$

$$= \left(\frac{3L}{4E^*R^2}\right)^{1/3}\frac{1}{\sqrt{\pi}\bar g}. \tag{12}$$

When expanding the right-hand side of equation (10) for model I into powers of $\kappa\tilde p$, the same leading-order linear term is obtained as for the mean-field approximation $A_{\rm PR}/\pi a_0^2$, namely the expression on the right-hand side of equation (5). However, at large loads, the asymptotic behaviors differ. The relative, complementary Hertzian contact area, $A_{\rm comp} \equiv 1 - A_{\rm real}/A_{\rm H}$, obeys depending on the model used

$$A_{\rm comp}({\rm PR}) \approx \frac{1}{\sqrt{\pi}}\exp\left\{-(2\kappa\tilde p/3)^2\right\} \tag{13}$$

$$A_{\rm comp}({\rm I}) \approx \frac{1}{2\kappa^2\tilde p^2} \tag{14}$$

for $\kappa\tilde p \gg 1$. Thus, the mean-field treatment of microscale roughness makes the contact area approach the continuum solution much faster than the refined approach of model I.

An improved alternative to mean field can be obtained by exploiting a relation for $A_{\rm rel}^{\rm flat}$ that is more accurate than equation (4). For example, a sum of two error functions weighted by a switching function $s(\bar p)$

$$A_{\rm rel}^{\rm flat}(\bar p) \approx \{1-s(\bar p)\}\,{\rm erf}(\tilde c_1\bar p) + s(\bar p){\rm erf}(\tilde c_2\bar p) \tag{15}$$

produces accurate contact area for randomly rough surfaces for different values of H and all loads outside the finite-size domains [9]. The $c_i \equiv \tilde c_i/E^*\bar g$ are constants, $c_1 = 1.9054$ and $c_2 = 1.4496$, and

$$s(\bar p) = {\rm erf}^2(\tilde c_2\bar p). \tag{16}$$

With this new estimate for $A_{\rm rel}^{\rm flat}$, we can no longer find a closed-form expression for the contact area of a nominally flat Hertz contact. However, the integral in equation (6) can be approximated by replacing $p_{\rm H}(r)$ in the switching function with $\bar p_{\rm H}$. This leads us to model II

$$A_{\rm II}(\tilde p) = \{1-s(\bar p_{\rm H})\}\,A_{\rm I}(\kappa_1\tilde p) + s(\bar p_{\rm H})A_{\rm I}(\kappa_2\tilde p) \tag{17}$$

with $\kappa_i = 2c_i/\sqrt{\pi}$. It shows similar asymptotic scaling as model I, however, with slightly altered coefficients: κ is replaced by κ_1 at small and by κ_2 at large loads.

3 Numerical methods

Numerical reference data are produced with the Green's function molecular dynamics (GFMD) method [14,4, 21]. Details of the method have been published numerous times and shall not be repeated here. Central aspects unique to the problem of the nominally flat Hertzian tip are nevertheless discussed in the following.

As usual, we exploit the small-slope approximation to combine the roughness of substrate and tip in a single height function $h(\mathbf{r})$, which is defined on the xy-plane. The height function is the sum of the "macroscopic" Hertzian contact geometry

$$h_{\mathrm{H}}(\mathbf{r}) = \frac{r^2}{2R} \tag{18}$$

and the microscopic roughness $h_{\mathrm{m}}(\mathbf{r})$, which is set up such that their Fourier transforms produce typical surface spectra [25]. To analyze the effect of microscopic roughness on the true contact area, we keep the load fixed and add different amounts of microscale roughness for a given random realization of h_{m} by choosing the combined roughness according to

$$h(\mathbf{r}) = h_{\mathrm{H}}(\mathbf{r}) + \lambda h_{\mathrm{m}}(\mathbf{r}). \tag{19}$$

The root-mean-square slope of $h_m(\mathbf{r})$ is normalized to one, while λ varies from very small to very large. By doing so, we exploit the observation by Pastewka and Robbins that the data produced for different systems can be superimposed when load is rescaled appropriately. This allows us to work with a single random realization. Since we implement all aspects of the small-slope approximation from the beginning, no precautionary measures have to be taken when λ becomes large. This is because we could rescale the height profile with a number that is sufficiently small for the small-slope approximation to be justified again. We could then also rescale L (or E^*) in such a way that we end up with a system for which the exact same equations would have to be solved as before.

One reason why we vary λ rather than load is that this course of action makes finite-size or finite-sampling effects — those due to a_{H} being a finite fraction of the linear system size — independent of λ. We thus always have the same value for the reference contact area in the continuum limit, which is very close but not exactly equal to the analytical expression. Another reason is that numerical scatter is reduced. This is because the same randomness is essentially sampled for each value of λ, or, in other words, for each reduced load. To make the sampling meaningful, one must ensure that the Hertzian contact radius encompasses a substantial amount of small-scale roughness. The way in which we attempt to achieve this is described next.

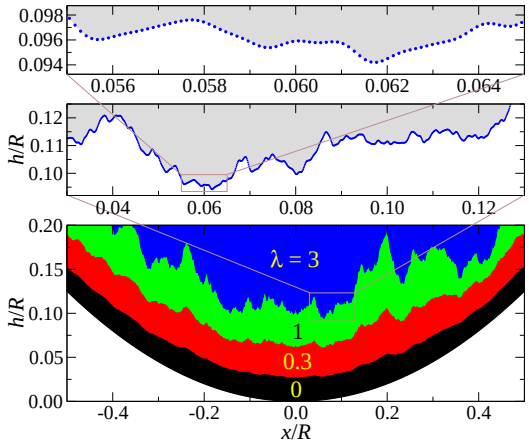

Fig. 1 Cross section through the height profile of undeformed tips at $y = 0$ for different amounts of micro-scale roughness as characterized by the scaling parameter λ. Final calculations are conducted at loads for which the smooth Hertzian contact radius would be $a_{\mathrm{H}} = 0.2$. Points in the topmost panel represent GFMD grid points at the lowest level of spatial resolution.

The radius of curvature defines the unit of length, i.e., $R = 1$. The load is chosen such that $a_{\mathrm{H}} = 0.2\ R$, which means that the Hertzian contact covers roughly 10% of the periodically repeated simulation area. The microscopic (default) substrate roughness is set up as follows: We use a Hurst roughness exponent of $H = 0.8$. The roll-off wave vector is set to $\lambda_{\mathrm{r}} = a_{\mathrm{H}}$, while the short wavelength cutoff is $\lambda_{\mathrm{s}} = a_{\mathrm{H}}/200$. This means that our contact radius samples over a little more than two decades of self-affine surface spectra. The GFMD layer is further discretized down to $\lambda_{\mathrm{s}}/8$ to ensure proximity to the continuum limit. The discretization is refined to $\lambda_{\mathrm{s}}/32$ for small values of λ. Lastly, h_{m} is normalized such that $\bar{g} = 1$. A cross section through the tip is shown in figure 1 for various values of λ.

From figure 1 one can see that initial contact does not necessarily occur at the center of the macroscopic tip center. For example, the lowest point of the $\lambda = 3$ tip lies about 0.06 R away from the macroscopic symmetry point. We abstain from discussing this and related extremely-small-load effects [19] further and instead refer to the excellent treatise of Pastewka and Robbins [20].

4 Results

We start our analysis with a representation of the relative, true Hertzian contact area, $A_{\mathrm{h}} \equiv A_{\mathrm{real}}/A_{\mathrm{H}}$, for the default systems having a contact radius 200 times the short-wavelength cutoff. Figure 2 reveals a quite convincing agreement between mean field and GFMD.

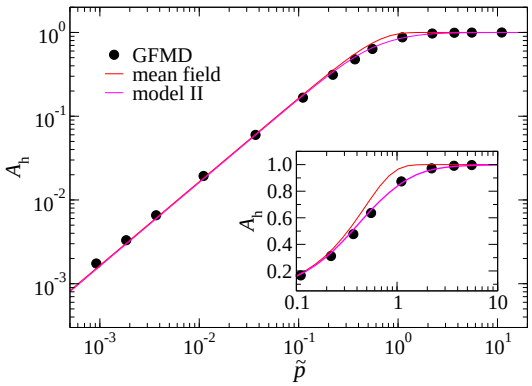

Fig. 2 Real, relative Hertzian contact area $A_\mathrm{h} = A_\mathrm{real}/A_\mathrm{H}$ as a function of reduced pressure $\tilde{p}$. Full circles show the results of GFMD simulations for which $a_\mathrm{H}/\lambda_\mathrm{s} = 200$. The red line represent the mean-field theory by Pastewka and Robbins for $\kappa = 2.2$, while the magenta line refers to model II, which is based on the area-load relation proposed in reference [9] without adjustment. The inset shows A_h on a linear scale.

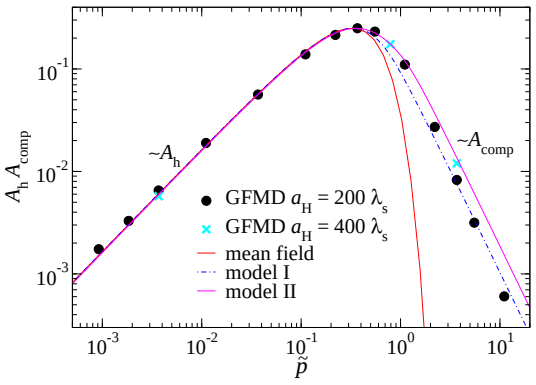

Fig. 3 The product $A_\mathrm{h} A_\mathrm{comp}$ as a function of reduced pressure $\tilde{p}$. Symbols are consistent with those used in figure 2. Moreover, (cyan) crosses refer to additional GFMD data encompassing more roughness scales than the default model. The dashed blue line shows results for model I with the same value of $\kappa = 2.2$ as mean field.

Results do not deviate by more than 10% in the shown regime. However, mean field slightly underestimates A_h when full contact is approached such that the relative errors of A_comp appear large. This trend is also revealed in the data of Pastewka and Robbins [20].

In order to better analyze how continuum Hertzian contact area is approached at large loads, the contact area data is presented in another form in figure 3. This reveals that A_comp decreases much too quickly with load in comparison to the numerically exact GFMD data. In fact, the analytical results discussed in the theory section are clearly borne out: mean field predicts A_comp to disappear exponentially with $\tilde{p}^2$, while the GFMD data is better described by a $\tilde{p}^{-2}$ scaling. The reason for this shortcoming of mean field can be rationalized as follows: Using $\bar{p}_\mathrm{H}$ instead of the spatially resolved $p_\mathrm{H}(r)$ leads to the neglect of non-contact area near the contact line. This is fixed in model I, which shows the correct scaling.

Since model I is based on an approximation that is not very accurate for nominally flat surfaces near full contact, non-negligible discrepancies occur at $0.5 \lesssim \tilde{p} \lesssim 1$, which lies near the cross-over from small to large loads. This last flaw is removed in model II.

It may be worth discussing some more details of the graph shown in figure 3. Finite-sampling effects, i.e., the cross-over to single-asperity contact mechanics, are not yet truly relevant for our (default) system at the smallest analyzed loads at which $A_\mathrm{h} \approx 0.001$. Sampling effects show up earlier at the large-load limit i.e., at A_comp of a few per cent. When sampling a more significant amount of disorder within the macroscopic Hertz contact by increasing $a_\mathrm{H}/\lambda_\mathrm{s}$, GFMD data approaches the predictions of model II, which thus is the most accurate out of the investigated models.

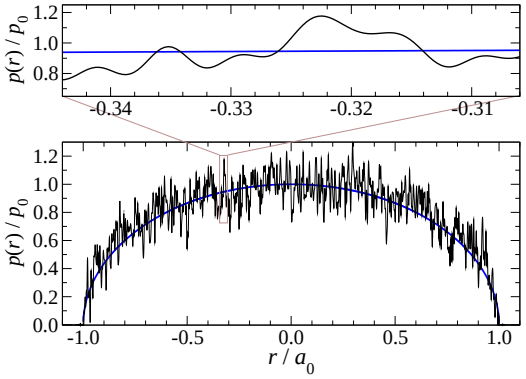

Fig. 4 Pressure profile for a Hertzian (thick blue line) and a nominally flat Hertzian contact (black line) at a reduced pressure of a $\tilde{p} \approx 3.5$ and for $a_\mathrm{H}/\lambda_\mathrm{s} = 200$.

Given the close approach of continuum theory and true contact area at large pressures, for example, at $\tilde{p} \approx 3.5$, one might be tempted to believe that the full calculation with roughness fluctuates only mildly around $p_\mathrm{H}(r)$ given in equation 1. Figure 4 reveals that this is not necessarily the case. It shows the pressure profile of a realization with $a_\mathrm{H}/\lambda_\mathrm{s} = 200$ and $\lambda = 0.03$. Its roughness is only one tenth of the red tip in figure 1, which already appears rather smooth to the naked eye.

5 Conclusions

In this work, we confirmed that the formula for the relative contact area in nominally flat Hertzian contact by Pastewka and Robbins [20] is very accurate and, in our opinion, sufficiently good for all practical purposes. The expression can yet be improved by abandoning the mean-field approximation. The advantage of the new formula — or an even more refined formula — is that the amount of non-contact within the Hertzian contact area is very precise, even at large loads. This result is insofar interesting, as it supports the central hypothesis underlying Persson theory, namely that the effects of small-scale roughness can be taken into account by first solving the contact mechanics problem at the large scale and by successively adding locally the effects of small-scale roughness into the calculation. Since the small-scale roughness induced non-contact lives predominantly near the contact line, the last statement also appears to hold reasonably well when pressure gradients are large, despite former criticism that Persson theory may be somewhat problematic for the (implicit) description of contact lines [16,9]. It remains to be seen to what extent this positive assessment of Persson theory persists when adhesion is included.

Acknowledgments The author gratefully acknowledges computing time on JUQUEEN at the Jülich Supercomputing Centre and the Deutsche Forschungsgemeinschaft for support through grant Mu 1694/5-1.

References

1. Akarapu, S., Sharp, T., Robbins, M.O.: Stiffness of contacts between rough surfaces. Phys. Rev. Lett. **106**, 204,301 (2011)
2. Almqvist, A., Campañá, C., Prodanov, N., Persson, B.N.J.: Interfacial separation between elastic solids with randomly rough surfaces: Comparison between theory and numerical techniques. J. Mech. Phys. Solids **59**, 2355–2369 (2011)
3. Bowden, F.P., Tabor, D.: Friction and Lubrication. Wiley, New York (1956)
4. Campañá, C., Müser, M.H.: Practical Green's function approach to the simulation of elastic semi-infinite solids. Phys. Rev. B **74**, 075,420 (2006)
5. Campañá, C., Müser, M.H.: Contact mechanics of real vs. randomly rough surfaces: A Green's function molecular dynamics study. EPL **77**, 38,005 (2007)
6. Campañá, C., Robbins, M.O., Müser, M.H.: Elastic contact between self-affine surfaces: comparison of numerical stress and contact correlation functions with analytic predictions. J. Phys.: Condens. Matter **20**, 354,013 (2008)
7. Cheng, S., Robbins, M.O.: Defining contact at the atomic scale. Tribol. Lett. **39**, 329–348 (2010)
8. Dapp, W.B., Lücke, A., Persson, B.N.J., Müser, M.H.: Self-affine elastic contacts: percolation and leakage. Phys. Rev. Lett. **108**, 244,301 (2012)
9. Dapp, W.B., Prodanov, N., Müser, M.H.: Systematic analysis of Persson's contact mechanics theory of randomly rough elastic surfaces. J. Phys.: Condens. Matter **226**, 355,002 (2014)
10. Hertz, G.: Ueber die Berührung fester elastischer Körper. J. reine angew. Math. **92**, 156–171 (1881)
11. Hu, X., Martini, A.: Atomistic simulation of the effect of roughness on nanoscale wear. Comput. Mater. Sci. **102**, 208–212 (2015)
12. Hyun, S., Pei, L., Molinari, J.F., Robbins, M.O.: Finite-element analysis of contact between elastic self-affine surfaces. Phys. Rev. E **70**, 026,117 (2004)
13. Johnson, K.L.: Contact Mechanics. Cambridge University Press, Cambridge University Press, UK (1985)
14. Karpov, E.G., J., G., Wagner, Liu, W.K.: A green's function approach to deriving non-reflecting boundary conditions in molecular dynamics simulations. Int. J. Num. Meth. Eng. **62**(9), 1250–1262 (2005)
15. Luan, B.Q., Robbins, M.O.: The breakdown of continuum models for mechanical contacts. Nature **435**, 929–932 (2005). DOI 10.1038/nature03700
16. Manners, W., Greenwood, J.A.: Some observations on persson's diffusion theory of elastic contact. Wear **261**, 600–610 (2006). DOI 10.1016/j.wear.2006.01.007
17. Mo, Y., Turner, K.T., Szlufarska, I.: Friction laws at the nanoscale. Nature **457**, 1116–1119 (2009). DOI 10.1038/nature07748
18. Mulakaluri, N., Persson, B.N.J.: Adhesion between elastic solids with randomly rough surfaces: Comparison of analytical theory with molecular-dynamics simulations. EPL **96**, 66,003 (2011)
19. Pastewka, L., Prodanov, N., Lorenz, B., Müser, M.H., Robbins, M.O., Persson, B.N.J.: Finite-size effects in contacts between self-affine surfaces. Phys. Rev. E **87**, 062,809 (2013)
20. Pastewka, L., Robbins, M.O.: Contact area of rough spheres: Large scale simulations and simple scaling laws. Appl. Phys. Lett. **xxx**(xxx), xxx–xxx (2016)
21. Pastewka, L., Sharp, T.A., Robbins, M.O.: Seamless elastic boundaries for atomistic calculations. Phys. Rev. B **86**, 075,459 (2012)
22. Persson, B.N.J.: Theory of rubber friction and contact mechanics. J. Chem. Phys. **115**, 3840–3861 (2001)
23. Persson, B.N.J.: Contact mechanics for randomly rough surfaces. Surf. Sci. Rep. **61**, 201–227 (2006)
24. Persson, B.N.J.: On the elastic energy and stress correlation in the contact between elastic solids with randomly rough surfaces. J. Phys. Condens. Matter **20**, 312,001 (2008)
25. Persson, B.N.J.: On the fractal dimension of rough surfaces. Tribol. Lett. **54**, 99–106 (2014)
26. Persson, B.N.J., Yang, C.: Theory of the leak-rate of seals. J. Phys. Condens. Matter **20**, 315,011 (2008)
27. Prodanov, N., Dapp, W.B., Müser, M.H.: On the contact area and mean gap of rough, elastic contacts: Dimensional analysis, numerical corrections and reference data. Tribol. Lett. **53**, 433–448 (2014)
28. Putignano, C., Afferrante, L., Carbone, G., G.Demelio: The influence of the statistical properties of self-affine surfaces in elastic contacts: A numerical investigation. J. Mech. Phys. Sol. **60**, 973–982 (2012)
29. Wenning, L., Müser, M.H.: Friction laws for elastic nanoscale contacts. Euro. Phys. Lett. **54**, 693–699 (2001). DOI 10.1209/epl/i2001-00371-6
30. Yastrebov, V.A., Anciaux, G., Molinari, J.F.: From infinitesimal to full contact between rough surfaces: Evolution of the contact area. Int. J. Solids Struct. **52**, 83 (2015)